

Theoretical Investigation into the Structural, Thermochemical, and Electronic Properties of the Decathio[10]circulene

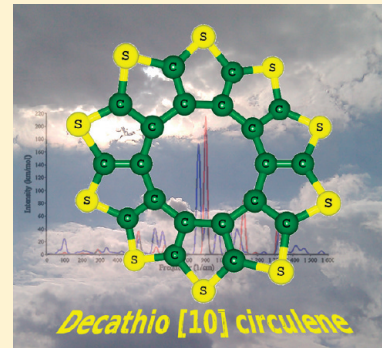
Brian Napolion,^{*,†} Frank Hagelberg,[‡] Ming-Ju Huang,[§] John D. Watts,[§] T. M. Simeon,[†] Derricka Vereen,[†] Wilbur L. Walters,[†] and Quinton L. Williams[†]

[†]Department of Physics, Atmospheric Sciences and Geoscience, Jackson State University, 1400 J. R. Lynch Street, P.O. Box 17660, Jackson, Mississippi 39217, United States

[‡]Department of Physics and Astronomy, East Tennessee State University, Johnson City, Tennessee 37614, United States

[§]Department of Chemistry and Biochemistry, Jackson State University, 1400 J. R. Lynch Street, P.O. Box 17910, Jackson, Mississippi 39217, United States

ABSTRACT: For the first time, a theoretical study has been performed on the prototypical decathio[10]circulene ($C_{20}S_{10}$) species, which is an analogue of the novel octathio[8]circulene “Sulfower” molecule ($C_{16}S_8$). Examinations of the singlet and triplet states of $C_{20}S_{10}$ were made at the B3LYP/6-311G(d) level. Local minima of C_2 and C_s symmetry were found for the lowest singlet and triplet states, respectively. The stability of $C_{20}S_{10}$ was assessed by calculating the ΔH°_f of $C_{16}S_8$ and $C_{20}S_{10}$ and the ΔH° for their decomposition into C_2S units. Frontier molecular orbital plots show that structural adjacent steric factors along with the twist and strain orientations of $C_{20}S_{10}$ do not disturb the aromatic π -delocalizing effects. In fact, $C_{20}S_{10}$ maintains the same p_z HOMO character as $C_{16}S_8$. These similarities are further verified by density-of-states characterization. Calculated infrared spectra of $C_{16}S_8$ and $C_{20}S_{10}$ show broad similarities. Molecular electrostatic potential results reveal that eight of the peripheral sulfur atoms are the most electronegative atoms in the molecule, while the interior ten-membered ring exhibits virtually no electronegativity.



1. INTRODUCTION

The chemical processes involved in the formation, production, and synthesis of novel materials continue to be mainstream focal points of contemporary scientific research. In particular, carbon–sulfur compounds are of major interest because of their use in electrical, optoelectronic, mechanical, and storage applications. These applications include photovoltaic (solar) cells,¹ light-emitting devices,² thin-film field-effect transistors,³ and hydrogen storage.⁴ To date, much research has focused on two groups of carbon–sulfur compounds: (1) oligothiophenes (formed from thiophene’s C_4S rings), a class of linked, chained, or bonded thiophene compounds that maintain a linear π -conjugated framework and (2) circulenes, a very rare class of cyclic compounds that are polyaromatic systems synthesized from arenes annulated into macrocycles. In other words, they are cyclic rings that are joined together to make other cyclic rings. Oligothiophenes (C_4S)_n are considered to be “self-assembling” molecules that can take many forms. The most notable two are flat linear or twisted helical geometries that possess a significant intermolecular interaction. This special annulated ring closure gives rise to a unique circulene compound, termed thiocirculenes.

For oligothiophene molecules, linear and helical orientations have received much attention in recent years. β -Oligothiophenes containing three, four, seven, and eleven fused rings, termed helicenes, have been studied quite extensively experimentally by Miyasaka, Rajca, and co-workers.^{5–7} In a series of reports by these authors, it is suggested that in oligomeric compounds

annulated thiophene rings are geometrically arranged to favor two- and three-dimensional associations when all sulfur atoms are positioned at the molecular periphery. One specific molecule, $C_{16}S_8$, octathio[8]circulene, popularly known as “sulfower” (sulfur + flower) is the first heterocyclic circulene to be synthesized, first accomplished by Chernichenko et al. in 2006.⁸ Although it differs from a conventional thiophene oligomer, it can be considered as such because of its unique cyclic “fused” structure. Several theoretical studies predict sulfower to exhibit a completely planar structure with D_{8h} symmetry.^{4,9,10} X-ray powder diffraction and solid-state ^{13}C NMR spectrometry have shown sulfower to possess a “near planar” configuration close to D_{8h} symmetry as proposed by computations.^{8,10} In the solid state, adjacent thin film column packs have close planar $S \cdots S$ contacts of roughly 3.25 Å and perpendicular $S \cdots S$ contacts of 3.9 Å.⁸ The close proximity of S atoms (due to its eight thiophene rings), large surface area ($\sim 56 \text{ \AA}^2$), and π -conjugated five-membered rings suggest that charge transport can be easily facilitated through the $C_{16}S_8$ sulfower molecule.¹¹ However, recent studies by Darling and Sternberg^{12,13} suggest some very important results that are applicable to strained thiopolymers such as oligothiophenes and twisted thiocirculenes presented in this study. They concluded: (1) charge transport, molecular band gap, ionization

Received: December 26, 2010

Revised: June 24, 2011

Published: June 27, 2011

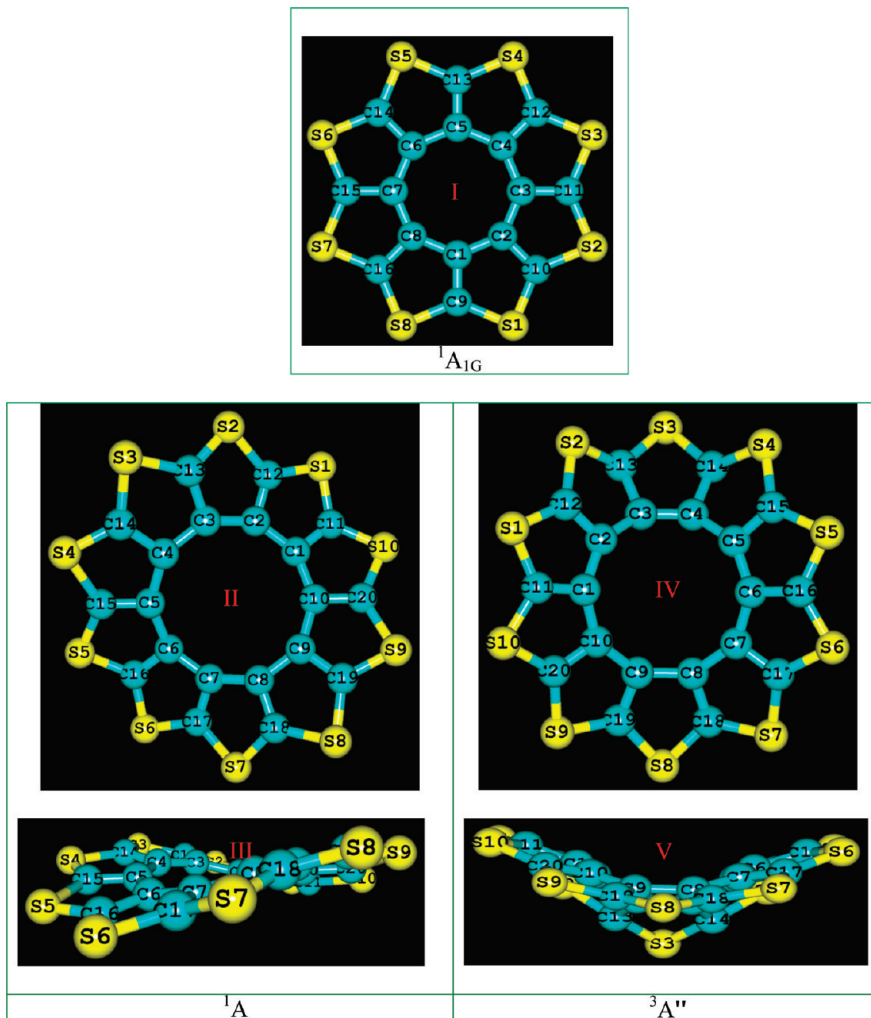


Figure 1. Optimized structures of $^1\text{A}_{1g}$ octathio[8]circulene (C_{16}S_8) and ^1A and $^3\text{A}''$ decathio[10]circulene ($\text{C}_{20}\text{S}_{10}$) at the B3LYP/6-311G(d) level. **I** displays planar octathio[8]circulene; **II** and **III** display the top and side views of the ^1A electronic state of decathio[10]circulene, respectively; and **IV** and **V** display the top and side views of the $^3\text{A}''$ electronic state of decathio[10]circulene, respectively.

energies, and other electrical properties are heavily influenced by the inner torsional angle (twist) between the pentagonal rings;^{12,13} (2) the dihedral disorder can reduce the conjugation length, thereby raising the HOMO–LUMO gap and reducing conductivity;¹³ and (3) although thiophenes may deviate from planarity, the p_z overlap is not necessarily destroyed in twisted and strained molecules.¹² These findings are significant for thiophene-derived structures such as $\text{C}_{20}\text{S}_{10}$ that are nonplanar and have a moderately strained geometric orientation.

Although octathio[8]circulene has been synthesized and characterized experimentally by Chernichenko et al.⁸ and Bukalov et al.,¹⁰ little is known about related thiocirculenes with more than eight thiophene rings. In fact, Chernichenko et al. stated that higher circulenes with more than eight rings such as nonathio[9]circulene appear to be promising candidates for synthesis. However, there seems to be significant difficulty in developing a systematic and rational experimental approach to synthesize these larger molecules,¹⁴ and theoretical approaches may provide insight. For instance, theory has been utilized concurrently to aid in the initial discovery of sulflower by estimating the stability of thiophenyl circulenes to choose the most stable conformation for synthesis of these cyclic compounds. Initially, DFT and the

resolution-of-the-identity MP2 (ri-MP2) methods were employed to derive stabilization strain energies of x -thio[x]circulenes ($x = 5–12$) as their total energy minus the sum of the energies of corresponding C_2S fragments.^{14,15} By plotting the strain energy versus the number of thiophenic units, one can draw several conclusions: (1) the minimum strain (twist or pucker) energies are found in thiophenyl circulenes that contain eight or nine thiophene rings, namely, octathio[8]circulene and nonathio[9]-circulene compounds; (2) decathio[10]circulene and undecathio-[11]circulene compounds have higher strain energies of ~ 5 and $7.5 \text{ kcal mol}^{-1}$; and (3) the strain energies of thiocirculenes that contain five, six, eleven, or twelve rings are significantly higher than those that contain 7–10 rings. Although theoretical calculations have already provided some insight with regard to the viability of thiocirculenes, several important questions have not been answered: (1) Is formation from C_2S the only reliable pathway to predict the stability of thiocirculenes? (2) Are larger circulenes (>9) feasible for synthesis despite their higher strain stabilization energies when compared to octathio[8]circulene? (3) Are there any thermochemical and kinetic models that can predict the viability of these thiocirculenes? (4) Is orbital symmetry maintained in twist and strain geometries as suggested

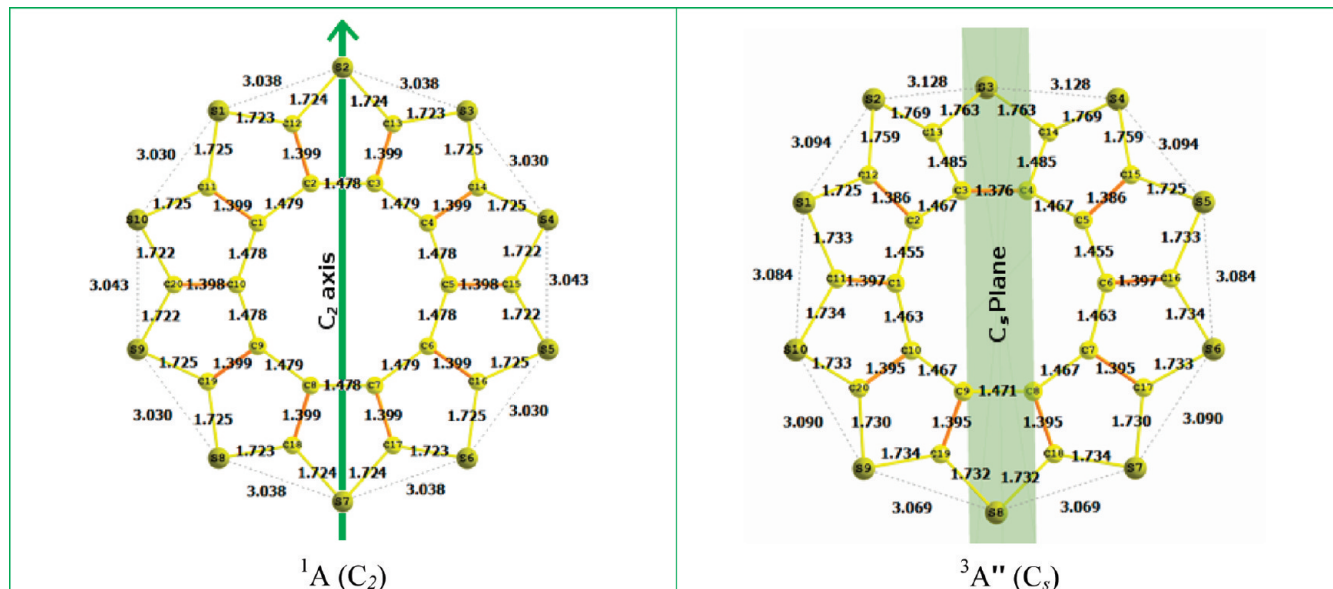


Figure 2. B3LYP/6-311G(d) geometrical parameters (\AA) of ^1A and $^3\text{A}''$ electronic decathio[10]circulene.

in other reports^{12,13} on similar thiophene molecules? Motivated by these questions and the prior theoretical prediction that decathio-[10]circulene is the most stable thiocirculene relative to octathio-[8]circulene,^{8,14} we decided to undertake this study to gain further insight into the structural, electrical, and thermochemical properties of this interesting molecule.

2. COMPUTATIONAL METHODS

Using the Gaussian 03 program,¹⁶ correlated electronic energies were computed via density functional theory (DFT) which has evolved as an advanced and robust computational method for the study of organosulfur compounds.^{12,13,17–19} For singlet and triplet decathio[10]circulene, geometries were optimized using the B3LYP functional^{20,21} in combination with the 6-311G(d,p) basis set. Second derivatives of the energy with respect to nuclear coordinates were evaluated to check whether stationary points are local minima and to obtain: (1) harmonic vibrational frequencies and (2) estimates of infrared (IR) intensities. Standard enthalpies (ΔH°) were acquired by using thermal corrections to the stationary point energies from the rigid rotor/harmonic oscillator/ideal gas approximation at the B3LYP/6-311G(d,p) level. Improved energies utilized in the ΔH_f° calculations were obtained by performing MP2(FC)/6-311G(d,p) and MP2(FC)/6-311G(2df,2pd) single-point calculations on the B3LYP-optimized geometries of octathio[8]circulene and decathio[10]-circulene. The following constraints were imposed in the optimization and frequency calculations: (1) tight optimization of geometrical parameters (rms criterion set to 10^{-6} au), (2) tight convergence of the self-consistent field (SCF) (10^{-8} au), and (3) ultrafine integration grid (95 radial shells and 590 angular points per shell).

Density-of-states (DOS) computations were performed by using DFT within periodic boundary conditions and in conjunction with a plane-wave basis set, as implemented in the Vienna ab initio Simulation Package (VASP) code.^{22–24} The generalized Kohn–Sham equations were solved utilizing a residual minimization scheme, namely, the direct inversion in the iterative subspace (RMM-DIIS) method.^{25,26} The interaction of valence

electrons and core ions was described by the projector-augmented wave (PAW) method.²⁷ In all DOS computations, the Perdew–Burke–Ernzerhof (PBE)²⁸ generalized gradient approximation (GGA) for the exchange-correlation functional was used. The B3LYP functional was not used in the DOS calculations since hybrid functionals can not be handled by the version of VASP to which we have access (version 4.6). Periodic boundary conditions were imposed on a cubic cell with dimension $20 \times 20 \times 40 \text{ \AA}^3$ for all the calculations. From inspection of the converged equilibrium geometries, the nearest-neighbor distance between atoms in adjacent supercells exceeds 12 \AA , making the interaction between supercells negligible. The molecular electrostatic potential (MEP) surfaces were generated using the Molekel program²⁹ at the B3LYP/6-311G(d) level using color depictions from red to blue to represent the spectrum of electronegative and electro-positive potential values.

3. RESULTS AND DISCUSSION

3.1. Structural Characterization. Figure 1 shows octathio-[8]circulene and the top and side views of singlet and triplet decathio[10]circulene. Initially geometries of singlet and triplet states of decathio[10]circulene ($\text{C}_{20}\text{S}_{10}$) were planar and constrained to maintain the highest point group symmetry, D_{10h} , during optimization. However, vibrational frequency calculations on the D_{10h} structures yielded a set of doubly degenerate imaginary frequencies for both singlet and triplet electronic states, implying that minima exist at lower point group symmetries. From there, the symmetry was lowered by displacing nuclei in directions that would lower the energy. The resulting structures were reoptimized, leading to stationary points with all real harmonic frequencies. A singlet structure with C_2 (^1A) point group symmetry and a triplet structure with C_s ($^3\text{A}''$) point symmetry were obtained.

The B3LYP/6-311G(d) geometrical parameters are depicted in Figure 2. The interatomic bond lengths vary slightly between the singlet and triplet structures. For the singlet, the distances between adjacent $\text{S} \cdots \text{S}$ atoms are $3.03\text{--}3.04 \text{ \AA}$ and slightly longer for the triplet, $3.07\text{--}3.13 \text{ \AA}$. For both species, the $\text{S} \cdots \text{S}$

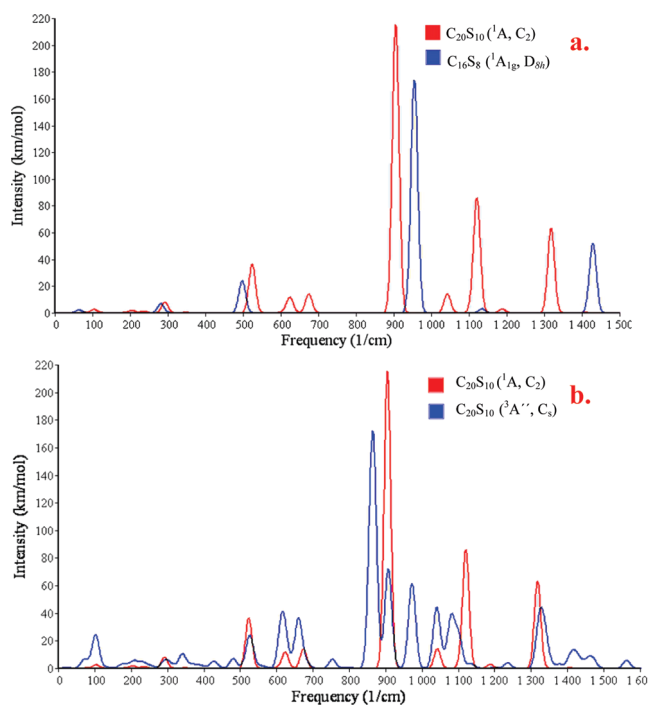


Figure 3. Theoretical infrared spectra of decathio[10]circulene and octathio[8]circulene at the B3LYP/6-311G(d) level. Frequencies range from 0 to 1600 cm^{-1} . (a) Represents ^1A decathio[10]circulene and $^1\text{A}_{1g}$ octathio[8]circulene. (b) Represents ^1A and $^3\text{A}''$ decathio[10]circulene. The spectra have been broadened by Lorentzians of bandwidth on one-half the height of 25 x -axis units.

distances are shorter than the corresponding distance experimentally obtained for octathio[8]circulene ($3.25\text{--}3.29\text{ \AA}$)^{8,10} and those obtained theoretically at the B3LYP/6-311G(d) level ($3.28\text{--}3.31\text{ \AA}$). Naturally, we would expect the distances between adjacent S atoms to be longer for octathio[8]circulene than for decathio[10]circulene because of predictions made by Dopper et al.³⁰ They theorized that if the sum of the sector angles in macrocyclic rings is close to 360° the system would be planar and exhibit no ring strain. Deviations from 360° lead to distortion from planarity, leading to quenched twisted “bowl and saddle” structures that place peripheral atoms closer together. In our case, this follows from the addition of more thiophene rings. The C–S bond lengths also vary little between singlet ($\sim 1.722\text{--}1.725\text{ \AA}$) and triplet ($\sim 1.725\text{--}1.770\text{ \AA}$) geometries, as do the C=C bond lengths. Comparing the C–S bond lengths of singlet decathio[10]circulene ($\sim 1.722\text{--}1.725\text{ \AA}$) with those of octathio[8]circulene obtained experimentally ($\sim 1.76\text{ \AA}$) and theoretically ($\sim 1.764\text{ \AA}$) at the B3LYP/6-311G(d) level, the values are in close proximity to one another, deviating at most by $\sim 0.039\text{ \AA}$. The C=C bond lengths are also similar: the calculated decathio[10]circulene values are $\sim 1.398\text{--}1.399\text{ \AA}$, while the experimental and theoretical octathio[8]circulene values are ~ 1.400 and $\sim 1.378\text{ \AA}$, respectively. On the whole, the geometrical parameters of the singlet decathio[10]circulene molecule are quite similar to the corresponding parameters of octathio[8]-circulene, suggesting the intramolecular forces of both molecules are of the same nature, although there is some torsion within the decathio[10]circulene molecule.

3.2. Vibrational Frequency and IR Analysis. Since decathio[10]circulene has yet to be isolated experimentally, theoretical IR

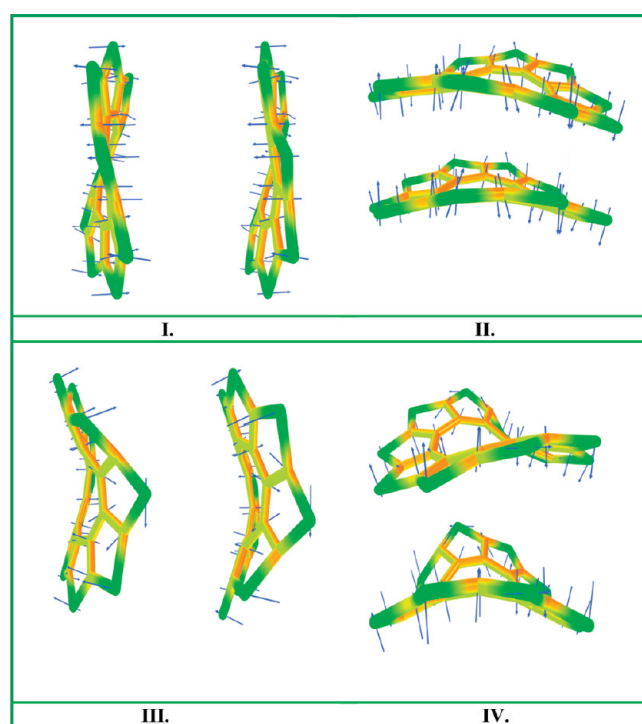


Figure 4. Horizontal and vertical views of the atomic displacement and restoring vectors after rotational projection of the force constants associated with normal mode vibration ω_1 at the B3LYP/6-311G(d) level. I and II represent ^1A decathio[10]circulene, and III and IV represent $^3\text{A}''$ decathio[10]circulene.

Table 1. Estimated Standard Heats of Formation (ΔH_f°) at 298 K of Gaseous C_{16}S_8 and $\text{C}_{20}\text{S}_{10}$ (kJ mol^{-1})

	C_{16}S_8		$\text{C}_{20}\text{S}_{10}$	
	pathway 1	pathway 2	pathway 1	pathway 2
B3LYP/6-311G(d,p)	1453	1236	1983	1711
B3LYP/6-311G(2df,2pd)	1199	1177	1667	1639
MP2/6-311G(d,p)	1163	633	1553	891
MP2/6-311G(2df,2pd)	445	653	674	935

spectroscopy is a valuable tool that can aid in the identification of this molecule. Notably, DFT vibrational spectra have been successfully used in recent works on similar molecules such as oligothienoacenes³¹ and thiophene³² and selenophene-derived heteroacenes³³ for identification. DFT calculations were also used in the assignment of the vibrational spectra of octathio[8]circulene.^{5,10} The B3LYP/6-311G(d)-predicted infrared spectra of singlet decathio[10]circulene and octathio[8]circulene are shown in Figure 3a. Those of singlet decathio[10]circulene and triplet decathio[10]circulene are shown in Figure 3b. Figure 4 displays the eigenvectors of decathio[10]circulene associated with the lowest-frequency normal mode vibrations, hereafter denoted as ω_1 .

Before discussing Figures 3 and 4, we anticipate that B3LYP/6-311G(d) is likely to provide a reasonable description of the vibrational spectra. For example, one can compare B3LYP/6-311G(d) results with the observed bands in the infrared spectrum of octathio[8]circulene reported by Bukalov et al.¹⁰ The

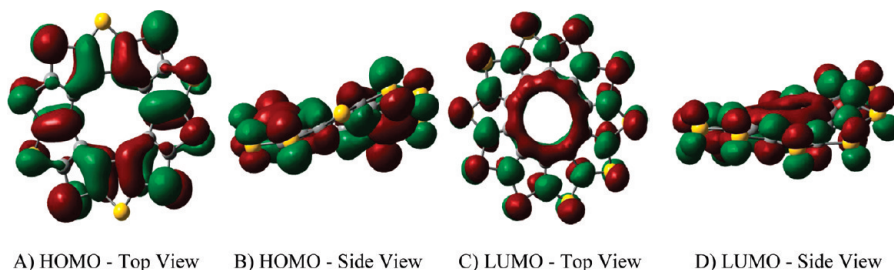


Figure 5. Frontier molecular orbital (FMO) isodensity plots of the HOMO and LUMO for singlet decathio[10]circulene ($C_{20}S_{10}$).

observed frequencies are 276, 501, 639, 933, 1110, and 1407 cm^{-1} . The features at 639 and 1110 cm^{-1} have very low intensities. The B3LYP/6-311G(d) frequencies (in cm^{-1}), along with intensities (in km mol^{-1}) and irreducible representations in parentheses, are 281 (7.1; E_{1u}), 497 (24.2; A_{2u}), 659 (0.0; E_{1u}), 955 (174.2; E_{1u}), 1133 (3.2; E_{1u}), and 1428 (52.5; E_{1u}). Given that the theoretical data are harmonic frequencies and that extending the basis set will slightly influence the results, this agreement is definitely satisfactory. The second A_{2u} mode, predicted by B3LYP/6-311G(d) to be at 63 cm^{-1} , is beyond the range of the experiment. Bukalov et al.¹⁰ also report DFT calculations that provide very good agreement with experiment.

Figure 3a shows the B3LYP/6-311G(d) infrared spectra of octathio[8]circulene and decathio[10]circulene. Superimposing the results for these molecules, one can view any specific characteristics that are common to both molecules. Since singlet decathio[10]circulene has C_2 symmetry, all 84 vibrational modes are infrared active. However, the vast majority have extremely low intensity. With two exceptions, all modes with significant intensity are those that correlate with the infrared-active modes in D_{10h} symmetry. In D_{10h} symmetry, the infrared-active modes of $C_{20}S_{10}$ are five E_{1u} and two A_{2u} modes, just as for D_{8h} $C_{16}S_8$.¹⁰ The normal coordinates for A_{2u} modes are motions perpendicular to the molecular plane, while they are in-plane motions for E_{1u} . On going to C_2 symmetry, the A_{2u} modes become B modes, while the E_{1u} modes split into A and B modes. Actually, the frequency difference between the A and B modes that come from the same E_{1u} mode is less than 1 cm^{-1} .

The peak of $C_{20}S_{10}$ at 1318 cm^{-1} consists of A and B modes. The normal coordinates primarily involve $\text{C}=\text{C}$ stretches, somewhat analogous to the band of $C_{16}S_8$ at 1429 cm^{-1} . The decrease in frequency correlates with the increase in $\text{C}=\text{C}$ bond length from $C_{16}S_8$ (1.378 \AA) to $C_{20}S_{10}$ (1.398 – 1.399 \AA). The peak for $C_{20}S_{10}$ at 1121 cm^{-1} also consists of A and B modes of identical frequencies. It is noteworthy that the intensity is much higher than that of the band of $C_{16}S_8$ at 1133 cm^{-1} . The band at 1042 cm^{-1} (B symmetry) does not derive from an infrared-active band in D_{10h} $C_{20}S_{10}$ and has no infrared-active counterpart in $C_{16}S_8$. For $C_{20}S_{10}$ there are A and B bands at 905 cm^{-1} of high intensity. The main motion is $\text{C}-\text{C}$ stretching. There is some similarity to the 954 cm^{-1} mode of $C_{16}S_8$. The decrease in frequency is consistent with the increase in $\text{C}-\text{C}$ bond length from $C_{16}S_8$ (1.423 \AA) to $C_{20}S_{10}$ (1.478 – 1.479 \AA). The $C_{20}S_{10}$ band at 675 cm^{-1} again consists of A and B modes and derives from an E_{1u} mode of D_{10h} $C_{20}S_{10}$. There is some significant $\text{C}-\text{S}$ stretching in the normal coordinate as the S atoms move toward and away from the center of the molecule. Although it is not visible in the spectrum, there is a corresponding E_{1u} band for $C_{16}S_8$ at 659 cm^{-1} , but its intensity is extremely low. The shift in

frequency on going from $C_{16}S_8$ to $C_{20}S_{10}$ is in line with the decrease in $\text{C}-\text{S}$ bond length (1.764 \AA ($C_{16}S_8$) and 1.722 – 1.725 \AA ($C_{20}S_{10}$)). The peak at 623 cm^{-1} is from A and B modes of $C_{20}S_{10}$ that do not correlate with an infrared-active mode of D_{10h} $C_{20}S_{10}$, and so there is no infrared-active counterpart in D_{8h} $C_{16}S_8$. The B mode of $C_{20}S_{10}$ at 524 cm^{-1} primarily involves movement of the carbon atoms perpendicular to the (approximate) plane of the molecule, with very little movement of S atoms. The corresponding band in $C_{16}S_8$ occurs at 497 cm^{-1} (A_{2u}).

For the triplet $C_{20}S_{10}$ (Figure 3b), there are ten peaks with intensities of 30 km/mol or higher. Many peaks are nearly identical with those of the singlet species with some either upshifted or downshifted.

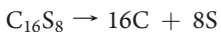
With respect to the lowest harmonic frequencies for the singlet and triplet structures, 2 and 20 cm^{-1} , respectively, the eigenvectors for those particular modes display a torsional motion, as shown in Figure 4. We note that although these torsional frequencies are low, the molecule is not fragile: these modes do not lead to dissociation or bond breaking. On the contrary, the bonding within the molecule is rigid, and there is significant cohesion within the molecule. The low-frequency mode moves the molecule toward the planar geometry, which is only slightly higher in energy: at the B3LYP/6-311G(d) level, the energy of the D_{10h} geometry is 4.4 kJ mol^{-1} ($1.05\text{ kcal mol}^{-1}$) above that of the C_2 geometry (singlet species). Hence, one low-energy pathway for interconversion of equivalent minima is via the planar geometry.

To gain further insight into the low-frequency modes, we investigated the frequency calculation output from the Gaussian Program, particularly the six low frequencies that correspond to the translations and rotations of the molecule. For well-converged structures, these frequencies should be very close to zero. This was the case for decathio[10]circulene, as all frequencies ranged from 0.047 to 1.127 cm^{-1} . Since some potential energy surfaces are especially flat when molecules go through internal translations and rotations, a low-frequency mode does not deem the molecule unstable. Similar trends in frequencies were found for other prototypical [10]circulenes³⁴ of the form $C_{10}N_{15}As_{15}F_{10}$, $C_{10}N_{15}Ga_{15}F_{10}$, and $C_{10}N_{10}B_{10}F_{20}$, where the ω_1 frequencies range from 1.4 to 8.4 cm^{-1} at the B3LYP/6-311G(d) level.

3.3. Thermochemical Properties. The heat of formation ΔH_f° of a compound is an essential quantity that strongly influences thermodynamic stability. In this study, the ΔH_f° (298.15 K) for decathio[10]circulene has been estimated by using two thermochemical pathways. Analogous calculations have been used to obtain the ΔH_f° for octathio[8]circulene to allow a comparison. Given the size of these molecules, highly accurate predictions cannot be expected, but at least

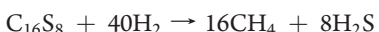
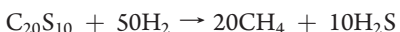
useful comparisons can be obtained. The strategies used are as follows:

Pathway 1: The calculated ΔH° values for the atomization reactions



were combined with experimental values of the ΔH_f° of C and S atoms to give the ΔH_f° of $\text{C}_{20}\text{S}_{10}$ and C_{16}S_8 .

Pathway 2: The calculated ΔH° values for the gas-phase reactions



were combined with experimental values of the ΔH_f° of CH_4 , H_2S , and H_2 to give the ΔH_f° of $\text{C}_{20}\text{S}_{10}$ and C_{16}S_8 .

The electronic energy differences were obtained from B3LYP/6-311G(2df,2pd) and MP2/6-311G(2df,2pd) energies at the B3LYP/6-311G(d) geometries. These energy differences were combined with B3LYP/6-311G(d,p) zero-point energies and thermal corrections to give ΔH° . The estimated ΔH_f° values of C_{16}S_8 and $\text{C}_{20}\text{S}_{10}$ are shown in Table 1. Evidently, there are large differences between the B3LYP and MP2 values for both compounds, with the B3LYP values being significantly larger. It is not immediately clear which estimates are best. However, it is likely that the B3LYP values are somewhat too high. In a study of ΔH_f° values of *n*-alkanes, Redfern et al.³⁵ found B3LYP significantly underestimated stability for the larger alkanes studied, reporting an error of more than 120 kJ mol⁻¹ for hexadecane. They suggested that "B3LYP has a significant problem with accumulation of errors as molecular size increases". Duan et al.³⁶ have also noted that DFT errors for ΔH_f° increase with increasing molecular size. Usually the calculated value is above the experimental value. Whether the MP2 values of ΔH_f° are more accurate than the B3LYP values is an open question. Although the present results do not permit prediction of ΔH_f° with any degree of certainty, they do provide a useful thermochemical comparison of C_{16}S_8 and $\text{C}_{20}\text{S}_{10}$. Certainly, $\text{C}_{20}\text{S}_{10}$ has a higher ΔH_f° , but the value is sufficiently small as to suggest that $\text{C}_{20}\text{S}_{10}$ is a viable species and might be observable.

Another comparison between C_{16}S_8 and $\text{C}_{20}\text{S}_{10}$ comes from the ΔH° for formation of these molecules from C_2S fragments: $10\text{C}_2\text{S} \rightarrow \text{C}_{20}\text{S}_{10}$ and $8\text{C}_2\text{S} \rightarrow \text{C}_{16}\text{S}_8$. A similar method using C_2S has been used for predicting the strain energy stabilities of thiocirculenes, indicating octathio[8]circulene to be most stable.^{8,14} Using MP2/6-311G(2df) energies and B3LYP/6-311G(d) zero-point energies and thermal corrections, the values of ΔH° are -5309 and -4342 kJ mol⁻¹ for forming $\text{C}_{20}\text{S}_{10}$ and C_{16}S_8 , respectively. These may be expressed as ΔH° values per C_2S unit of -530.9 and -542.8 kJ for $\text{C}_{20}\text{S}_{10}$ and C_{16}S_8 , respectively. These data suggest that although C_{16}S_8 is more stable than $\text{C}_{20}\text{S}_{10}$, the difference is not huge and $\text{C}_{20}\text{S}_{10}$ is likely to be a viable species. This is consistent with calculated estimates of strain energies of these species that predict octathio[8]circulene to be closest in energy to decathio[10]circulene.^{8,14} Finally, using the calculated ΔH° values for forming C_{16}S_8 and $\text{C}_{20}\text{S}_{10}$ from C_2S , the ΔH° for the process $\text{C}_{20}\text{S}_{10} \rightarrow \text{C}_{16}\text{S}_8 + 2\text{C}_2\text{S}$ is 967 kJ mol⁻¹.

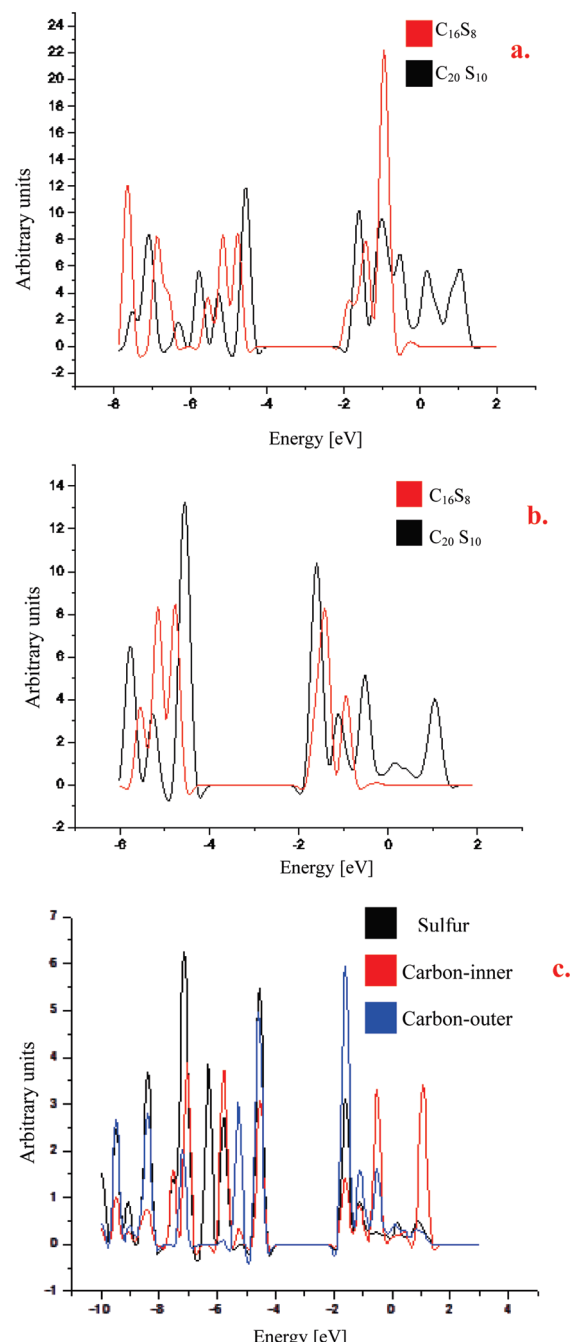


Figure 6. (a) Total DOS distributions for C_{16}S_8 (red) and $\text{C}_{20}\text{S}_{10}$ (black) in the exact vicinity of the HOMO–LUMO gap. (b) Partial DOS distributions for C_{16}S_8 (red) and $\text{C}_{20}\text{S}_{10}$ (black) in the exact vicinity of the HOMO–LUMO gap. Only the contributions of p_z symmetry are included. (c) DOS distributions of p_z symmetry for various groups of $\text{C}_{20}\text{S}_{10}$ constituents. The assignment of line colors to groups of atoms is as follows: black represents all S atoms; red represents all atoms of the inner C_{10} ring; and blue represents all atoms of the outer C_{10} atoms.

3.4. Frontier Molecular Orbital and Density of States (DOS) Analysis. The frontier molecular orbital (FMO) isodensity plots in Figure 5 demonstrate that the HOMO of singlet decathio[10]circulene is predominately composed of delocalized p_z orbitals, as is the HOMO-1 orbital. Although the singlet structure contains a slight concavity, the π orbitals seem to

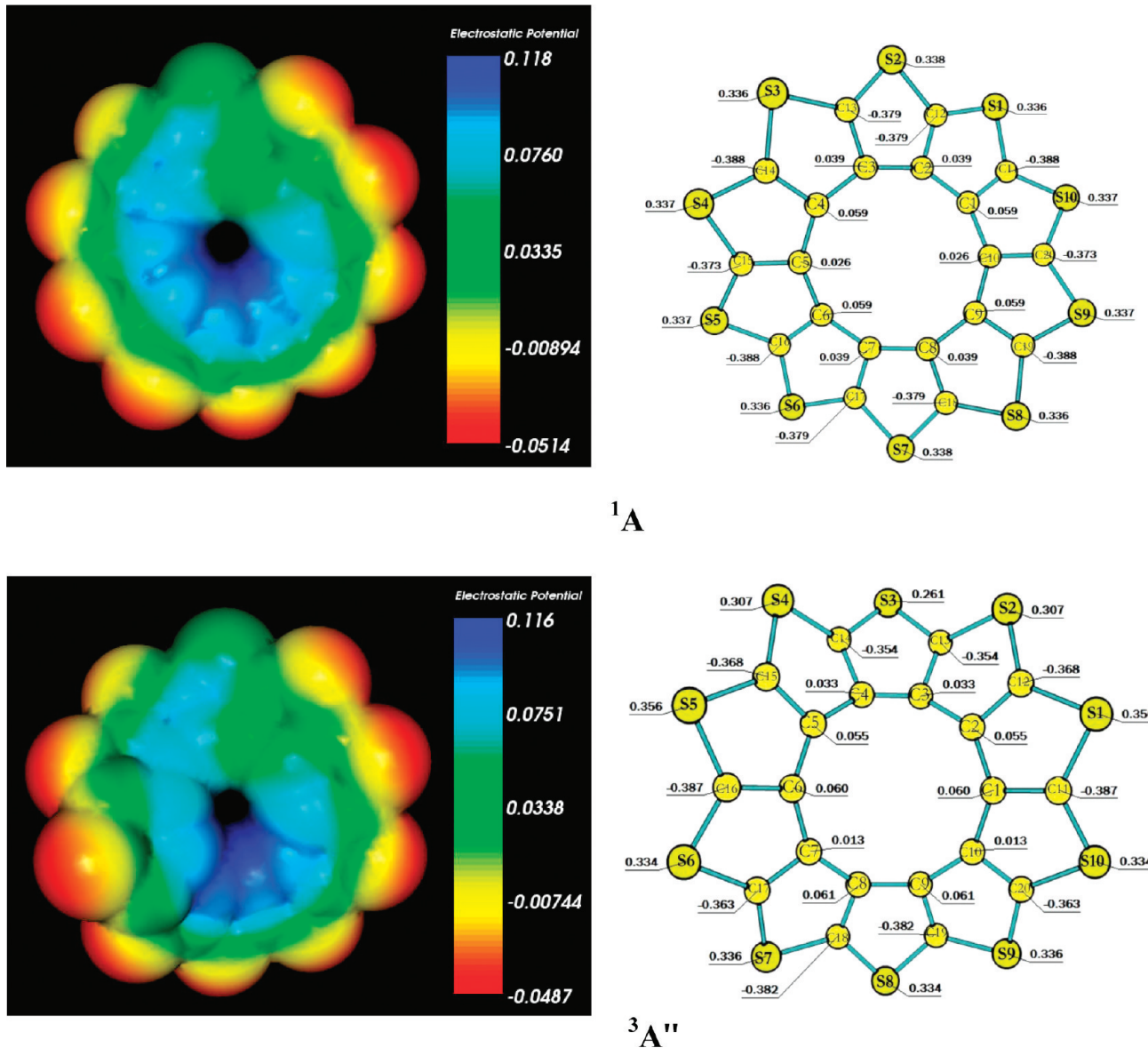


Figure 7. Electrostatic potential maps at the solvent accessible surface generated for the ¹A and ³A'' electronic states of decathio[10]circulene colored by the molecular electrostatic potentials (MEPs) at the B3LYP/6-311G(d) level. The highest (electropositive) and lowest (electronegative) values are indicated in the corresponding scale by red and blue colors, respectively. The ball-stick models shown to the right have the same geometry as the MEP surfaces. Figures to the right represent the Mulliken charges for the respective molecules to the left.

contribute equally to both the convex and concave regions of the molecule. These FMO results suggest that decathio[10]circulene is not strongly affected by “twist” and has significant aromatic character, like octathio[8]circulene. This is very significant in that Darling¹² contradicted prior assumptions that breaking planarity corresponded to broken conjugation of π orbital symmetry in polythiophene molecules. The results in this study uphold his predictions that orbitals can remain evenly distributed within an oligomer in spite of torsion within the molecule. In terms of the LUMO, a high degree of delocalization is found within the interior ten-membered carbon ring, while the thiophene rings exhibit more localized molecular orbitals. With reference to conductivity, the energy difference between the HOMO and the LUMO (ΔE_{H-L}) can be considered a first approximation to the band gap energy. At the B3LYP/6-311G(d) level, the HOMO–LUMO gap (ΔE_{H-L}) of singlet decathio[10]circulene

is 4.37 eV. Compared to the gap of octathio[8]circulene, 4.67 eV, this suggests that decathio[10]circulene is slightly more conductive. For the triplet state, the energy gap between the highest singly occupied molecular orbital (HSOMO) and the lowest singly occupied molecular orbital (LSOMO), ΔE_{SH-LS} , is 2.41 eV at the B3LYP/6-311G(d) level.

Figure 6 shows total and partial DOS distributions characteristic for the C₁₆S₈ and the C₂₀S₁₀ spin singlet in two different representations. Specifically, the total DOS distributions for the two species are compared in Figure 6(a). In accordance with the frontier orbitals shown in Figure 5, the plane-wave method yields a marked predominance of p_z states in the vicinity of the energy gap (see Figure 6(b)). As this procedure tends to underestimate the size of the gap, the plane-wave result ($\Delta E = 2.90$ eV) is lower than the HOMO–LUMO energy difference (4.37 eV, see above) found when employing the Gaussian basis.

The plane-wave treatment, however, yields an energy gap of very considerable size as well. The p_z contributions of selected groups of $C_{20}S_{10}$ constituents to the DOS are presented in Figure 6(c). Three groups are distinguished, namely all S atoms as well as the ten atoms of the inner and the outer C_{10} ring. The maxima bounding the energy gap are composed of all three contingents, in keeping with the character of the HOMO and LUMO orbitals. The two peaks adjacent to the maximum that corresponds to the HOMO reflect the asymmetry between the two characteristic C_{10} rings that determine the structure of $C_{20}S_{10}$. Thus, the lower peak (at -5.75 eV) displays hybridization between the S atom subsystem and the inner C_{10} ring. The corresponding peak due to the outer C_{10} ring, however, is shifted by 0.48 eV to higher energy which may be interpreted as a signature of the increased strain experienced by the outer ring in comparison to the inner.

3.5. Molecular Electrostatic Potential (MEP) Surfaces. The molecular electrostatic potential (MEP) surfaces of 1A and $^3A''$ decathio[10]circulene obtained at the B3LYP/6-311G(d) level are plotted in Figure 7. For decathio[10]circulene, we observe that there are slight differences in the MEPs between the two electronic states (i.e., singlet vs triplet), while there are some overwhelming similarities. There are significant areas of negative electron density, particularly around the perimeter near the sulfur atoms. Eight of the peripheral sulfur atoms are most electronegative relative to the other atoms within the molecule. These distinguishable sites suggest that the formation of another bond with sulfur with multiple functional groups is viable if these atoms are acting as electron donors. In the case of the two remaining sulfur atoms, we observe a slightly decreased electrostatic potential or electron depletion at the sites (S2) and (S3). Another interesting observation is the substantially decreased electrostatic potential in the region of the twisted C–C–C bond for $^3A''$, when the angle of that bond is decreased from $(143.2^\circ/{}^1A)$ to $(139.4^\circ/{}^3A'')$, indicated by the darker blue region in the molecule. Conversely, the interior cyclic ten-membered ring is overwhelmingly electropositive for both electronic states, which is consistent with the more positive Mulliken charges localized in that region. This suggests this particular interior region is electron deficient, and this area could in fact accept electrons from strong donors at inner circumference sites (C atoms). Nonetheless, the MEPs of both 1A and $^3A''$ seem to be excellent indicators of the molecule's chemical reactivity, primarily because there are significant regions of electron depletion (electrophilic) and accumulation (nucleophilic).

4. CONCLUSION

Although decathio[10]circulene is not planar, its properties seem to coincide with octathio[8]circulene. We have computationally designed a heteroanalogue of octathio[8]circulene, namely, decathio[10]circulene. In the absence of experimental data, this theoretical study provides significant information leading to deeper insight into the architecture of sunflower derivatives that would not be ordinarily known. Relative to octathio[8]circulene, our theoretical results suggest this molecule is potentially viable as indicated by the close proximity of the: (1) geometrical parameters; (2) vibrational spectra assignments describing signature bond stretches and other motions; and (3) the thermochemical stability implied by the enthalpy of formation calculations. We further note that DOS and FMO calculations reflect aromatic character that is also consistent with octathio[8]circulene, regardless of steric factors that are present in the decathio[10]circulene equilibrium

structures. MEP contour plots signify this species has a significant electronegativity difference due to the large polarization in charges, and there are substantial variations in the electron density localized within different regions of the molecule (i.e., interior ring region versus exterior ring region). Future studies will include exploring the series $C_{20+2j}S_{10+j}$, with emphasis on the stability variation and in particular the strain enhancement as a function of j with more rigorous electron correlation methods.

■ ACKNOWLEDGMENT

This work was supported by the Department of Defense through the U.S. Army/Engineer Research and Development Center (Vicksburg, MS)—Contract #W912HZ-10-C-0107, the Office of Naval Research Grant # N00014-09-1-0980, the Jackson State University-Corning Partnership, and the U.S. Department of Education's Integrated Learning and Teaching Environment (ILTE) Grant # P120A080014. F.H. acknowledges support from the Tennessee NSF-EPSCoR Grant, "TN-SCORE". Ming-Ju Huang acknowledges support from the JSU NSF-CREST grant (HRD-0833178). A very special debt of gratitude goes to Dr. Mehri Fadavi and Dr. P.C. Yuan for providing additional hardware and other computing equipment used to conduct this research. Q.L.W. gives a most appreciable thanks to Josiah Dosunmu for his continuous assistance, laborious technical support, and unrelenting commitment to the needs, concerns, and requirements of our research group with the HPCDNM cluster at Jackson State University. We also acknowledge Fredrick McFarland for working in our group.

■ REFERENCES

- Lee, A. W. M.; Yeung, A. B. W.; Yuen, M. S. M.; Zhang, H.; Zhao, X.; Wong, W. Y. *Chem. Commun.* **2000**, 75.
- Perepichka, I.; Perepichka, D.; Meng, H.; Wudl, F. *Adv. Mater.* **2005**, 17, 2281.
- Sun, Y.; Liu, Y.; Zhu, D. *J. Mater. Chem.* **2005**, 15, 53.
- Datta, A.; Pati, S. K. *J. Phys. Chem. C* **2007**, 111, 4487.
- Miyasaka, M.; Rajca, A. *J. Org. Chem.* **2006**, 71, 3264.
- Miyasaka, M.; Rajca, A. *J. Am. Chem. Soc.* **2005**, 127, 13806.
- Rajca, A.; Pink, M.; Wang, H.; Rajca, S. *J. Am. Chem. Soc.* **2004**, 126, 15211.
- Chernichenko, K. Y.; Sumerin, V. V.; Shpanchenko, R. V.; Balenkova, E. S.; Nenajdenko, V. G. *Angew. Chem.* **2006**, 45, 7367.
- Gahungu, G.; Zhang, J.; Barancira, T. *J. Phys. Chem. A* **2009**, 113, 255.
- Bukalov, S. S.; Leites, L. A.; Lyssenko, K. A.; Aysin, R. R.; Korlyukov, A. A.; Zubavichus, J. V.; Chernichenko, K. Y.; Balenkova, E. S.; Nenajdenko, V. G.; Antipin, M. Y. *J. Phys. Chem. A* **2008**, 112, 10949.
- Mohakud, S.; Pati, S. K. *J. Mater. Chem.* **2009**, 19, 4356.
- Darling, S. B. *J. Phys. Chem. B* **2008**, 112, 8891.
- Darling, S. B.; Sternberg, M. *J. Phys. Chem. B* **2009**, 113, 6215.
- Chernichenko, K. Y.; Balenkova, E. S.; Nenajdenko, V. G. *Mendeleev Commun.* **2008**, 18, 171.
- Dadvand, A.; Ciciora, F.; Chernichenko, K. Y.; Balenkova, E. S.; Osuna, R. M.; Rosei, F.; Nenajdenko, V. G.; Perepichka, D. F. *Chem. Commun.* **2008**, 5354.
- Frisch, M. J.; Trucks, G. W.; Schlegel, H. B.; Scuseria, G. E.; Robb, M. A.; Cheeseman, J. R.; Montgomery, J. A., Jr.; Vreven, T.; Kudin, K. N.; Burant, J. C.; Millam, J. M.; Iyengar, S. S.; Tomasi, J.; Barone, V.; Mennucci, B.; Cossi, M.; Scalmani, G.; Rega, N.; Petersson, G. A.; Nakatsuji, H.; Hada, M.; Ehara, M.; Toyota, K.; Fukuda, R.; Hasegawa, J.; Ishida, M.; Nakajima, T.; Honda, Y.; Kitao, O.; Nakai, H.; Klene, M.; Li, X.; Knox, J. E.; Hratchian, H. P.; Cross, J. B.; Bakken, V.; Adamo, C.; Jaramillo, J.; Gomperts, R.; Stratmann, R. E.; Yazyev, O.;

Austin, A. J.; Cammi, R.; Pomelli, C.; Ochterski, J. W.; Ayala, P. Y.; Morokuma, K.; Voth, G. A.; Salvador, P.; Dannenberg, J. J.; Zakrzewski, V. G.; Dapprich, S.; Daniels, A. D.; Strain, M. C.; Farkas, O.; Malick, D. K.; Rabuck, A. D.; Raghavachari, K.; Foresman, J. B.; Ortiz, J. V.; Cui, Q.; Baboul, A. G.; Clifford, S.; Cioslowski, J.; Stefanov, B. B.; Liu, G.; Liashenko, A.; Piskorz, P.; Komaromi, I.; Martin, R. L.; Fox, D. J.; Keith, T.; Al-Laham, M. A.; Peng, C. Y.; Nanayakkara, A.; Challacombe, M.; Gill, P. M. W.; Johnson, B.; Chen, W.; Wong, M. W.; Gonzalez, C.; Pople, J. A. *Gaussian 03*, revision C.02; Gaussian, Inc.: Wallingford, CT, 2004.

- (17) Jeffries-EL, M.; Sauvé, G.; McCullough, R. D. *Adv. Mater.* **2004**, *16*, 1017.
- (18) Griesel, S. J. H.; Lackinger, M.; Jamitzky, F.; Market, T.; Hietschold, M.; Heckl, W. M. *Langmuir* **2004**, *20*, 9403.
- (19) Cao, H.; Ma, J.; Zhang, G.; Jiang, Y. *Macromolecules* **2005**, *38*, 1123.
- (20) Becke, A. D. *Phys. Rev. A* **1988**, *38*, 8822.
- (21) Lee, C.; Yang, W.; Parr, R. G. *Phys. Rev. B* **1988**, *37*, 785.
- (22) Kresse, G.; Hafner, J. *Phys. Rev. B* **1993**, *47*, 558.
- (23) Kresse, G.; Hafner, J. *Phys. Rev. B* **1994**, *49*, 14251.
- (24) Kresse, G.; Furthmüller, J. *Comput. Mater. Sci.* **1996**, *6*, 15.
- (25) Wood, D. M.; Zunger, A. *J. Phys. A* **1985**, *18*, 1343.
- (26) Pulay, P. *Chem. Phys. Lett.* **1980**, *73*, 393.
- (27) Bloechl, P. E. *Phys. Rev. B* **1994**, *50*, 17953.
- (28) Perdew, J. P.; Burke, K.; Ernzerhof, M. *Phys. Rev. Lett.* **1996**, *77*, 3865.
- (29) Flükiger, P.; Lüthi, H. P.; Portmann, S.; Weber, J. *Swiss Center for Scientific Computing, Manno (Switzerland)* 2000–2001.
- (30) Dopfer, J. H.; Oudman, D.; Wynberg, H. *J. Am. Chem. Soc.* **1973**, *95*, 3692.
- (31) Osuna, R. M.; Zhang, X.; Matzeger, A. J.; Hernandez, V.; Navarrete, J. T. L. *J. Phys. Chem. A* **2006**, *110*, 5058.
- (32) Osuna, R. M.; Ortiz, R. P.; Hernandez, V.; Navarrete, J. T. L.; Miyasaka, M.; Rajca, S.; Rajca, A.; Glaser, R. *J. Phys. Chem. C* **2007**, *111*, 4854.
- (33) Osuna, R. M.; Ortiz, R. P.; Okamoto, T.; Suzuki, Y.; Yamaguchi, S.; Hernandez, V.; Navarrete, J. T. L. *J. Phys. Chem. B* **2007**, *111*, 7488.
- (34) Gribanova, T. N.; Zefirov, N. S.; Minkin, V. I. *Pure Appl. Chem.* **2010**, *82*, 1011.
- (35) Redfern, P. C.; Zapol, P.; Curtiss, L. A.; Raghavachari, K. *J. Phys. Chem. A* **2000**, *104*, 5850.
- (36) Duan, X.-M.; Song, G.-L.; Li, Z.-H.; Wang, X.-J.; Chen, G.-H.; Fan, K.-N. *J. Chem. Phys.* **2004**, *121*, 7086.